Proceedings of ASME Turbo Expo 2011
GT2011
June 6-10, 2011, Vancouver, British Columbia, Canada

GT2011-46172

A METHOD FOR THEORETICAL PREDICTION OF FREQUENCY SCATTER RANGES FOR FREESTANDING FORGED STEAM TURBINE BLADES

Thomas Grönsfelder[1]
Siemens AG – Energy Sector
LP Steam Turbine Development
Mülheim/Ruhr, Germany

Thomas.Groensfelder@
siemens.com

Alexander Hofbauer
Siemens AG – Energy Sector
LP Steam Turbine Development
Mülheim/Ruhr, Germany

Alexander.Hofbauer@
siemens.com

Christoph H. Richter
Siemens AG – Energy Sector
LP Steam Turbine Development
Mülheim/Ruhr, Germany

Christoph-Hermann.Richter@
siemens.com

ABSTRACT

Large steam turbine end stage rotating blades are commonly manufactured by forging and machining to the final geometry. As in every manufacturing process certain geometric tolerances have to be granted. In particular, the allowed tolerances on the airfoil geometry do have a significant influence on the natural frequencies of the final blades.

The resulting frequency scatter is appreciated in terms of mistuning the whole ring of blades, as an adequate mistuning has shown advantages under unstalled flutter conditions. An excessively large band is not acceptable, due to the fact that the blade frequencies are tuned to not-coincide with harmonic multiples of the rotor speed under stationary operation.

This paper describes a theoretical method for prediction of a manufactured blade design frequency scatter, based only on nominal geometric information about the blade. Therefore, it is suited to be used during the development of a blade without having a prototype produced. The method is divided into three different steps. First, a numerical experiment is performed creating a number of geometrically modulated FE models. These models are used in a calculation of natural frequencies. Second, these frequencies serve as input for an identification of a simple algebraic representation of the frequencies. This allows a fast calculation by interpolation without the need to process the FE models. Third, the identified simplified equation is used in conjunction with different optimization algorithms for analysis of the specific design characteristics.

The validity of the chosen matrix equation is shown by comparison to the FE calculations, before different blade types are investigated. Characteristics and options of the implemented optimization routines are discussed. Finally, the comparison of differently tuned blade types are used to demonstrate the capabilities of the described algorithm.

NOMENCLATURE

Δf_i	Frequency difference to nominal geometry at same operation speed for *i*-th mode
ΔF_i	Frequency difference of the *i*-th mode for one geometry at different operation speeds
$\Delta\vec{x}$	Vector of geometric modification data
$\vec{l}$	Vector term of the simplified equation
$\vec{G}$	Gradient of a scalar function
$\underline{H}$	Hessian matrix of a scalar function
$\underline{Q}$	Matrix term of the simplified equation
dh	Normalized thickening variation between two adjacent radial cross sections
h_0	Maximum thickening
k_f	Relative frequency deviation factor
l_i	Relative frequency lift at different rotor speeds
n	Total number of free parameters in $\vec{l}$ and $\underline{Q}$
N	Number of geometry modifications
od	Over determination factor
r	Residual for least squares fit

ABBREVIATIONS

FE	Finite Element
LSB	Last Stage Blade
LSF	Least Squares Fit
SEQ	Simplified System of Equations

[1] Corresponding author

INTRODUCTION

Figure 1 shows a large freestanding last stage blade (LSB). An overview of design intends for current developments is given in [1]. Common radial heights L for 50 Hz applications of the developed designs is about and above 1000mm.

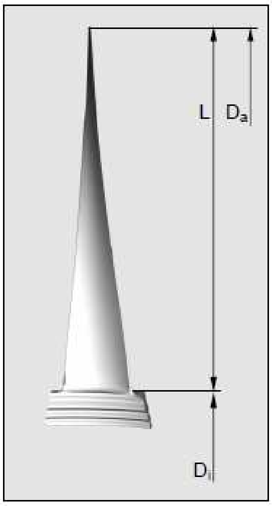

FIGURE 1 IMAGE OF A LAST STAGE BLADE

Manufacturing of such blades usually starts with forging of raw material to a geometry having a certain amount of oversize. From this, the two options grinding or milling are used for machining to the final airfoil geometry, while the geometry of the blade attachments is usually milled. In particular the tolerances which have to be granted for machining of the airfoil geometry can significantly influence the natural frequencies of the final blade. This more or less random distribution of mass over the airfoil surface leads to a natural frequency scatter even if a batch of blades are manufactured on the same machines. The observed frequency scatter therefore is a sensitive indicator for deviations in the manufacturing process. Thus the frequency measurements of the final blades at standstill are an important part of the quality assurance of the manufacturing process.

The fact that blade tuning has a major effect to blade fatigue behavior is widely accepted. An adequate strategy to assure safe designs is to avoid resonance at rated speed, i.e. coincidence of blade natural frequencies and speed harmonics of the rotor. In [2] a tuning up to the 8^{th} rotor harmonic frequency is demanded. The frequency spread of manufacturing induced uncertainties was estimated based on empiric data and is also included to the Campbell diagrams of [2], see Fig. 2. This natural frequency scatter is appreciated in terms of mistuning the whole ring of blades, since adequate levels o mistuning have shown advantages under unstalled flutter conditions, [3]. On the other hand, mistuning may lead to unwanted amplitude magnification in the forced response [4]. In addition, an excessively large frequency scatter is not acceptable as it can even inhibit resonance-free operation at rated speed.

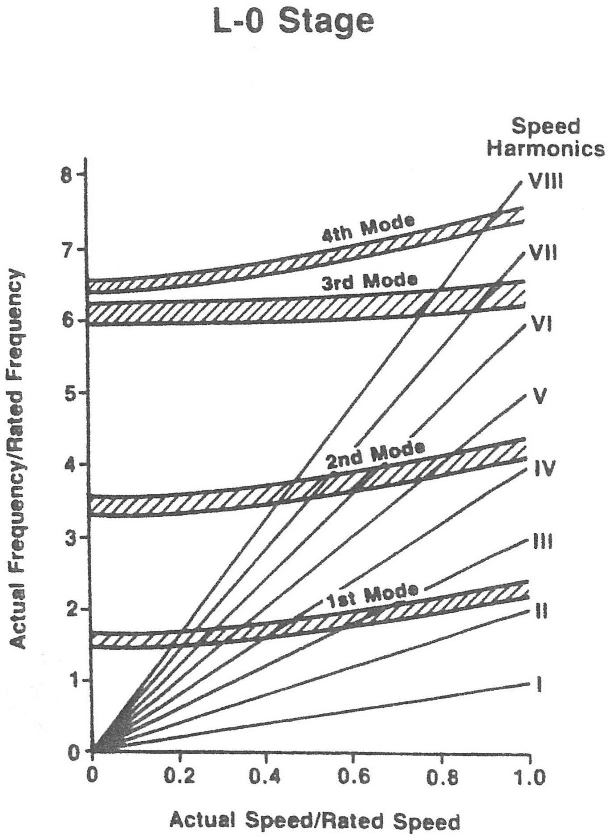

FIGURE 2 CAMPBELL DIAGRAM OF A LAST STAGE BLADE [2]

The authors of [5] investigated the possible reduction of lifetime of hot combustion turbine components using a parametric CAD model and a probabilistic modeling. Another probabilistic approach, this time for the prediction of static and dynamic frequencies was described in [6]. The authors implemented a procedure combining a neural network and a Monte Carlo simulation. The training process for the neural network variables was done here using a parametric FE model of a rather generic shaped model of a turbine blade.

The method proposed with this paper uses an analytical equation for modeling of the underlying effects. The structure of the paper follows the steps to be taken for conduction of the analyses. Firstly, the required numerical experiment is described. Secondly, the mathematical model and the identification of free model parameters is shown. Thirdly, embedding of the mathematical model into different levels of optimization routines leads to a calculation procedure to be used for prediction of frequency scatter or identification of allowable tolerances. Following this, certain aspects for application of the method are investigated and validated against FE calculations. The paper concludes with an application of the proposed methodology to different blade geometries and comparison of results. It will be shown that the frequency scatter is a unique property of each blade design. Using the described procedure, frequency scatter as a design characteristic can be predicted during development, leading to increased quality and reduced development time.

THEORY AND MODELING

The starting point for the work was a parametric FE model that has proven to provide reliable and accurate frequency predictions in low pressure (LP) blade development for many years, Fig. 3.

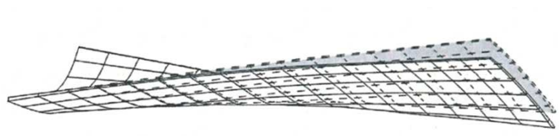

FIGURE 3 FE MODEL OF AN AIRFOIL AND FIRST MODE

This model is based on a building block approach dividing a blade into the functional components

- fir-tree root and steeple section of the shaft
- airfoil

Each of the components is defined by basic geometry data files, e.g. hub radius or outer diameter, which are compiled to the final FE model. The airfoil geometry is defined by a number of cross sections on constant radial height. These sections are designed during development to meet the aerodynamic requirements of the airfoil. Following this, the FE model is created by radial connection of adjacent cross sections and definition of the actual FE mesh entities. A basic prerequisite for the described procedure are the interfaces for manipulation of the nominal cross sections.

A straightforward approach to the described target would be a direct combination of the FE model with an optimization algorithm searching for a maximum (resp. minimum) frequency deviation. Obviously, such an optimization using the full FE model would lead to unpredictable computational efforts, which is unacceptable during development of new blades. The main idea to the solution of this problem was a combination of a fixed number of FE calculations with the identification of simplified algebraic representation of the effects.

Usually, experimental system identification is used for building mathematical models for dynamic systems [7]. Following this idea the procedure is divided into the steps

- Conduction of a numerical experiment using a FE model leading to a predictable computational effort. In following steps the calculated frequencies are treated as experimental data.
- Identification of the system parameters for a simplified system of equations (SEQ) using a least square fit method.
- Analysis of the design characteristics by application of optimization routines to the SEQ, e.g. prediction of frequency scatter.

Numerical Experiment

A basic requirement for the numerical experiment is the capability of the calculation method to model the influence of slight geometric modifications to the natural frequencies. Long term experience in blade development with the underlying FE model has proven that the frequency predictions provide the required accuracy to fulfill this demand. On the other hand, an optimal reduction of computational effort is reached when the required modification parameters in the FE model are limited to a minimum. The minimum number of model parameters is defined by a number of radial cross sections and one parameter to be modified on each of the sections. The simplest possible parameter is the modification defined by a constant thickening on the surface of the cross section shown in Fig. 4.

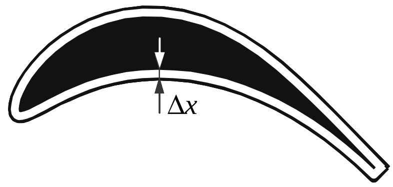

FIGURE 4 MODIFICATION OF THE PROFILE CROSS SECTION

Two parameters would offer the possibility to apply different thickening on pressure and suction side or defining a linear distribution. In order to realize the minimum computational effort, it was here decided to stay with the first level approach using one variable per cross section.

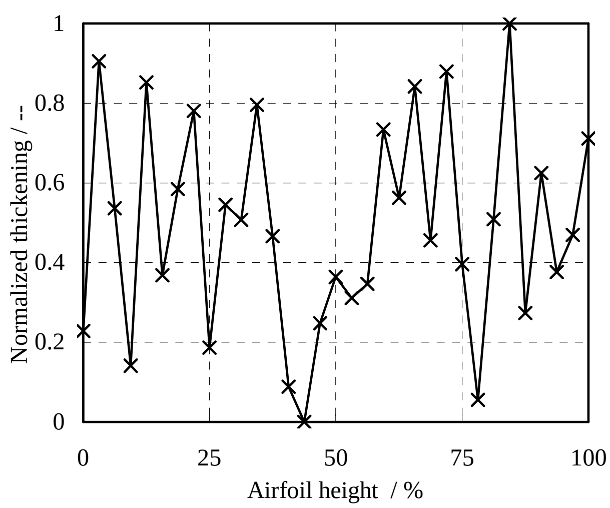

FIGURE 5 VISUALIZATION OF THE GEOMETRIC MODIFICATIONS

The implementation of the numerical experiment is divided into several steps. A set of geometry modification data files is created using random functions. These values are scaled to span a range of geometric spread, which is defined by the tolerance limits. A visualization of a possible random modification vector $\Delta\vec{x}$ is shown in Fig. 5. An automatic computational procedure is used to conduct the steps

- Creation of the input data using the basic modification files.
- FE model creation and conduction of the calculation.
- Extraction and storage of the desired data.

The advantage of the chosen procedure is the fully predictable computational effort for the FE calculations.

Simplified Equation

A common approach for approximation of an arbitrary function in the vicinity of a point of interest is the application of a Taylor-series representation

$$F(x-x_0) \approx \sum_{i=0} a_i \cdot (x-x_0)^i \tag{1}$$

with the parameters a_i identified from the partial derivative of the function $F(x)$ evaluated at x_0. According to the behavior of the function to be described the series is often restricted to linear, quadratic or cubic order.

Applying a grey-box approach of system identification theory [7], the shape of the modeling equation has to be postulated in advance and the parameters have to be identified from experimental data and algebraic calculations. For the given problem the geometry modification is described by the vector $\Delta\vec{x}$ and the function to be approximated is the scalar frequency deviation from the nominal natural frequency

$$\Delta f = f - f_{\text{nominal}} \qquad (2).$$

Thus, the simplified equation has to be of vector type. Postulating a sufficient accuracy by reduction to 2nd order, the equation can be written

$$\Delta f = \vec{l} \cdot \Delta\vec{x} + \Delta\vec{x}^T \underline{Q}\, \Delta\vec{x} \tag{3}$$

or alternatively in index notation

$$\Delta f = l_i \cdot \Delta x_i + q_{kl} \cdot \Delta x_k \Delta x_l \tag{4}$$

Where $\vec{l}$ is a vector of the size of $\Delta\vec{x}$ and $\underline{Q}$ is a square matrix of the size of $\Delta\vec{x}$ in each direction. It is shown later that the postulated shape sufficiently models the effect of the thickening on the natural frequencies. A more general description of the polynomial modeling is given in [7].

Obviously, a unique set of equations is required for each approximated natural frequency. Nevertheless, the desired parameters in $\vec{l}$ and $\underline{Q}$ can be identified from the results of the same geometrically modified FE calculations.

In order to get a further reduction of the system parameters in $\vec{l}$ and $\underline{Q}$ it was assumed that the $\underline{Q}$-matrix is of symmetric shape. With this applied to Eq. (3) it can be found that $\underline{Q}$ can be treated as triangular shaped, including the main diagonal. With N defining the size of $\Delta\vec{x}$ the number of free parameters n in $\vec{l}$ and $\underline{Q}$ can be calculated to

$$n = 2N + \frac{N\cdot(N-1)}{2}\,. \tag{5}$$

Using Eq. (5) it can be seen that an increased number of geometry modifications significantly increases the number of required calculations for parameter identification. A nonuniform thickening using two different values on suction and pressure side would double the value of N. With 35 radial sections n would increase with a factor of 3.84 from 665 to 2555.

Parameter Identification

The next step is the combination of the simplified equation Eq. (3) and the calculation results of the numerical experiment. The calculated frequency differences Δf, the related vectors of geometric deviation $\Delta\vec{x}$ and the structure of Eq. (3) are input for the parameter identification procedure. Combining the unknown constant parameters in $\vec{l}$ and $\underline{Q}$ with the results from the *m*-th FE calculation the *m*-th residual is defined by

$$r_m = \Delta f_m - l_i \cdot \Delta x_{im} - q_{kl} \cdot \Delta x_{km} \Delta x_{lm} \tag{6}$$

The task for identification of unknown parameters is a common problem for experimental system identification. Usually a Least Squares Fit (LSF) of the form

$$Minimize\, F(\vec{p}) = \sum_{i=1}^{m} r(\vec{p})_m{}^2 \tag{7}$$

is applied for solving this kind of problems. A commercial optimization routine was used for this implementation. It was designed for finding an unconstrained minimum of a sum of squares of m nonlinear functions in n variables ($m \geq n$). As the function is known, a gradient

$$G_i = \frac{\partial r}{\partial p_i} \tag{8}$$

and Hessian matrix

$$H_{ij} = \frac{\partial^2 r}{\partial p_i \partial p_j} \tag{9}$$

of the problem - regarding the parameters p in $\vec{l}$ and $\underline{Q}$ - for each equation m can be supplied to the routine explicitly.

After successful parameter identification, the SEQ can be used for efficient prediction of geometry induced frequency deviations. Different options for using this SEQ for further design analysis are shown below. The accuracy of the predictions and related requirements for overdetermination for the least square fit was investigated thoroughly. Results are shown below.

Calculation of Frequency Scatter

The calculation of frequency scatter is a straightforward application using the SEQ. For this task a routine for constrained minimization is used. A schematic outline of the procedure is shown in Fig. 6.

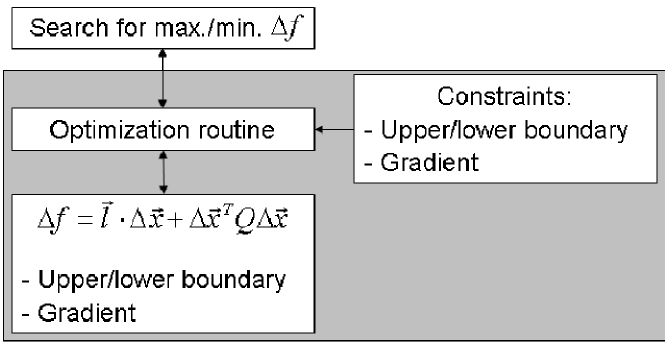

FIGURE 6 PROCEDURE FOR SEARCHING FOR FREQUENCY SCATTER

For an increased computational efficiency the gradient

$$G_i = \frac{\partial \Delta f}{\partial \Delta x_i} \tag{10}$$

and the Hessian-matrix

$$H_{ij} = \frac{\partial^2 \Delta f}{\partial \Delta x_i \partial \Delta x_j} \tag{11}$$

- regarding the variation of $\Delta\vec{x}$ - are again calculated and supplied to the algorithm. As the physical limits of the described problem is of constrained type, the frequency optimization routine has to be of constraint type, too.

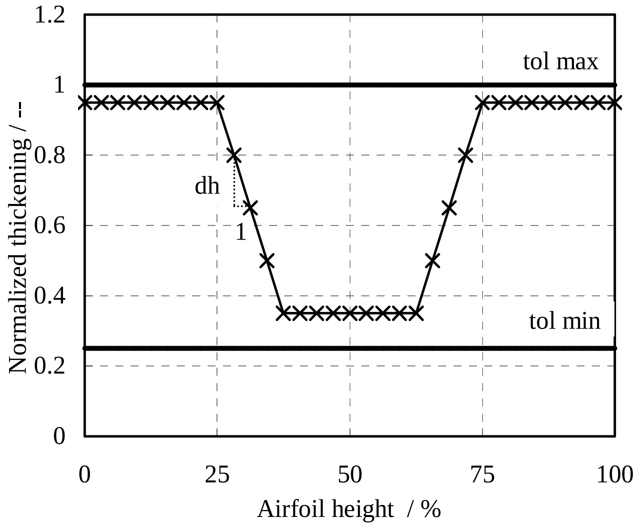

FIGURE 7 DEFINITION OF CONSTRAINTS

Figure 7 shows an example of the applied constraints. The thick full lines specify an upper and lower limit as design space for the optimization algorithm.

An additional constraint

$$dh = \frac{x_{i+1} - x_i}{h_0} \tag{12}$$

for the thickening difference at adjacent sections in $\Delta\vec{x}$ was introduced, Fig. 7. It is motivated empirically, as an unconstraint optimization for *dh* would result in jumps from the upper to the lower boundary limit and vice versa to achieve a maximum absolute frequency deviation (“bang-bang shape”). Such final geometry is possible but not very likely to occur in a machining process and it is leading to an unrealistically large predicted frequency scatter. Thus, the limitation was added in order to derive a procedure which is capable to predict maximum as well as likely frequency scatter.

A meaningful calibration for *dh* is required for productive application of the method. As a side effect, this calibration can be used to cover the uncertainty introduced by the constant thickening of the underlying FE models. With these findings, the constant thickening was identified to deliver sufficient accuracy for the tolerance prediction by requiring a minimized computational effort.

Tolerance Optimization

The geometric boundary constraints are useful in several ways. It is possible to restrict scatter of a single frequency by specifying a geometry. For example, the minimum possible deviation for a first natural frequency can be effectively influenced if the tolerance in the tip area is tightened, since this shape is similar to a simple bending beam shape.

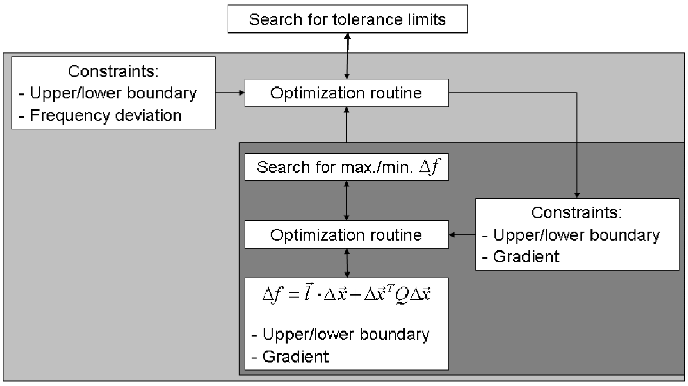

FIGURE 8 TOLERANCE OPTIMIZATION

For large blades more than one frequency is to be tuned, Fig. 1. Therefore, a further development level was created. With another optimization routine wrapped around the frequency scatter calculation, the tolerance to fit predefined frequency limits can directly be designed (Fig. 8). Here the outer optimization routine modifies the geometric boundaries of the previously described inner routine.

RESULTS

Accuracy of the Simplified Equation

Basic mathematics says that there are at least n equations required for identification of n parameters in Eq. (3). In case of $m > n$ the system is overdetermined by the factor

$$od = \frac{m}{n} \tag{13}$$

and a least squares fit can be performed. The required input data is derived from the number of calculations in the numerical experiment.

The accuracy of the predictions made with Eq. (3) is expected to increase with increasing number of overdetermination. This expectation is only valid if the postulated shape of Eq. (3) provides an appropriate description of the physical effects. To check this behavior a blade geometry was freely chosen, which is not contained in the pool of the LSF data.

Figure 9 shows the reduction of the prediction error by increasing the overdetermination of the first six natural frequencies. An increased overdetermination leads to a reduced error for all natural frequencies. The errors for the first six natural frequencies converge to below 0.1Hz at an over determination of approximately 1.7. Using the mentioned 35 radial cross sections, this corresponds to approximately 1100 FE calculations to be conducted prior the parameter identification. The factor was verified using different blade designs and geometry modification calculations.

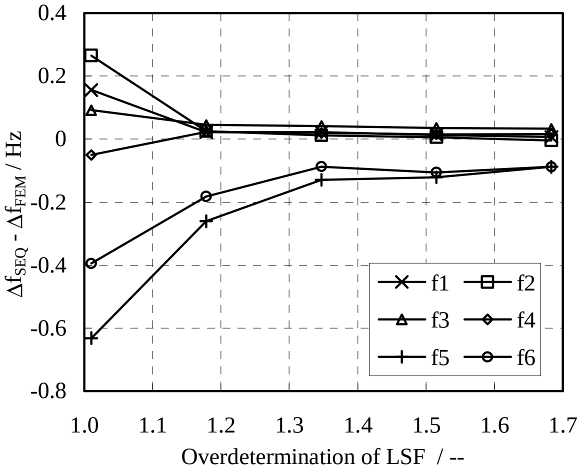

FIGURE 9 ACCURACY OF PREDICTION VERSUS OVERDETERMINATION

The described accuracy can safely be assumed to be sufficient for the desired application. Therefore, the number of required calculations in the numerical experiment for later application of the procedure was fixed to this value.

Influence of the Optimization Boundaries

The limitation of the maximum geometric thickening, Fig. 7, obviously restricts the maximum as well as the minimum predicted frequency deviation. A lower boundary of the design space for the optimization routine further reduces the range of achievable upper and lower frequency deviations. The limitation of *dh* leads to the same result of an even more reduced frequency band.

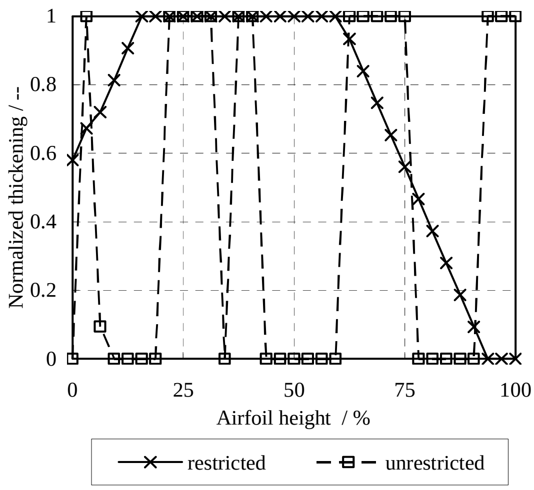

FIGURE 10 OPTIMIZATION RESULT FOR MAX. F_1 DEVIATION WITH AND WITHOUT RESTRICTION

Figure 10 shows the geometry identified for a maximum deviation of a first mode with and without restriction of the gradient *dh*. It is clearly visible that the optimization routine follows the underlying mathematical rules and creates the already described bang-bang shape, while the restricted optimization creates a far smoother geometry.

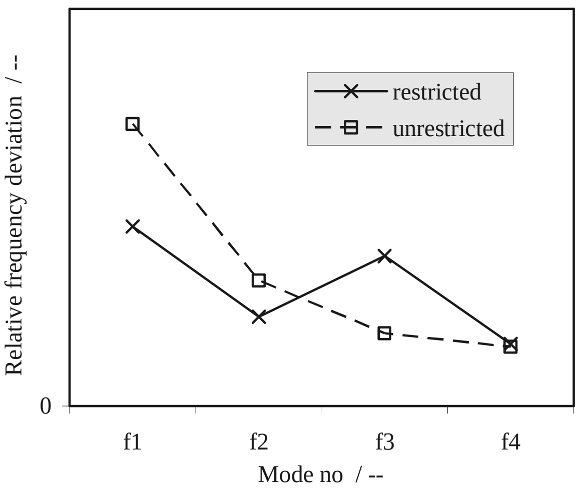

FIGURE 11 INFLUENCE OF RESTRICTION ON OPTIMIZATION RESULT

The effect of these geometries on the derived frequencies is shown in Fig. 11, using the definition

$$k_f = \frac{f_i - f_{i,\text{nominal}}}{f_{i,\text{nominal}}} \tag{14}$$

of the relative frequency deviation factor.

Due to the comparable shapes of the first and second mode, the effect on the second mode is similar to the first one, but not as strong. In contrast to this, the third mode is raised for the optimization using a *dh*-constrained geometry. This behavior is not an indication of an error, as only the first frequency was target function of the geometry optimization. Similar results could be obtained with other modes being subject for the optimization.

Influence of the Blade Root

The parametric building block FE model provides the option to omit the blade root from the calculation. The physical effect of a calculation without root can be visualized by the simple example of a bending beam. As the root represents additional elastic material, a calculation with a fixed lower end of the beam results in raised frequencies. The question then arises if this effect is also visible in the SEQ-predicted relative frequency differences?

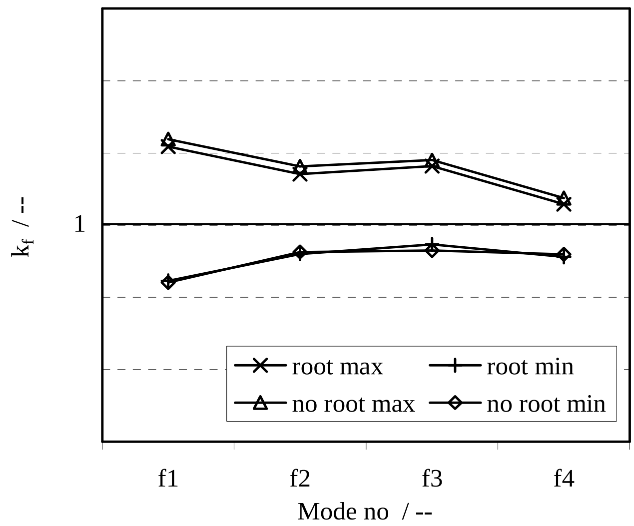

FIGURE 12 COMPARISON OF RESULTS INCLUDING THE BLADE ROOT

Two different pools of FE calculations were set up. One with and the other without the blade root. Figure 12 shows an example result for this investigation, using the same parameters for optimization. Obviously, the lower end of the expected frequency band is less affected than the maximum values of the band. Nevertheless, the overall bandwidth of the reduced FE model includes the predicted bandwidth of the full model. At least for the f_1, this behavior can be explained easily with the simplified model of a bending beam by variation of the clamping stiffness and assumed thickness distribution for a high or low frequency deviation, respectively.

It can be concluded that a calculation without root reduces computational effort and tends to provide conservative results.

Frequency Lift by Centrifugal Load

Large steam turbine blades generate raising natural frequencies during speed up, usually shown in a Campbell diagram of Fig. 1. This well known phenomenon is mainly driven by stress stiffening due to the centrifugal load. This section discusses the influence of geometric variations to the frequency lift behavior.

Data From the Numerical Experiment The frequency lift

$$\Delta F_i = f_{i,\text{rated}} - f_{i,\text{standstill}} \tag{15}$$

of a specific geometry can be investigated directly using the FE calculation results. This is only valid if the same geometry input to the FE model for standstill and rated speed calculation was used. Fulfilling this prerequisite, the relative lift deviation from the nominal frequency lift can be calculated using

$$l_i = \frac{\Delta F_\mathrm{i} - \Delta F_{i,\mathrm{nominal}}}{\Delta F_{i,\mathrm{nominal}}} \quad (15)$$

for each frequency of all of the *i*-th FE geometry model.

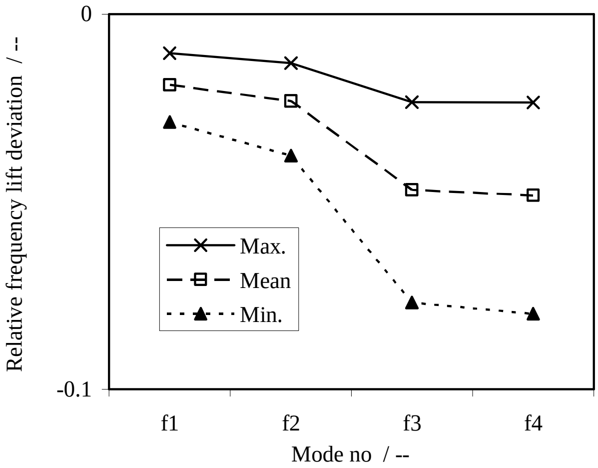

FIGURE 13 RELATIVE FREQUENCY LIFT DEVIATION FOR BLADE DESIGN A

Figure 13 shows the minimum, mean and maximum relative frequency lift deviation from the nominal geometry frequency lift for the first four natural frequencies. All values being lower than zero means that the lift for the nominal geometry is the highest one for all of the evaluated models. This result is interesting, as some of the frequencies are higher in standstill than for the nominal geometry. And it may lead to the speculation that also the lift may be higher for these geometries.

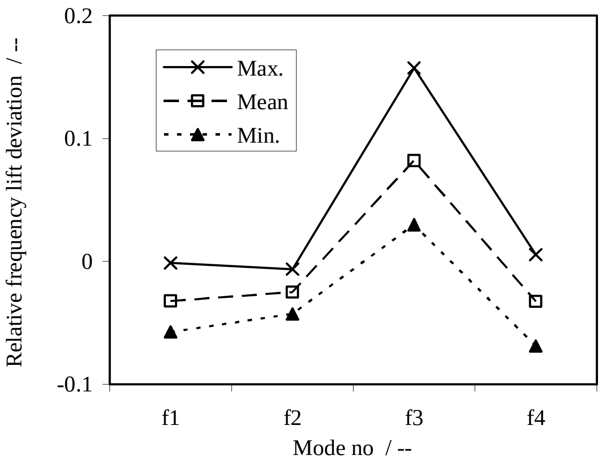

FIGURE 14 RELATIVE FREQUENCY LIFT DEVIATION FOR BLADE DESIGN B

The same graph for a different blade design revealing a different behavior is shown in Fig. 14. While the first, second and fourth frequency behave in a similar way for both designs, the third mode generates a frequency lift which is larger than the nominal one. From this, it can be stated that each blade design has a characteristic footprint in the developed frequency scatter.

Optimized Results from the SEQ As the pool of geometry modification used for the numerical experiment and for the results shown in Fig. 13 and Fig. 14 is created randomly, it does probably not contain the geometries leading to the maximum/minimum frequency deviation for all modes. These geometries are delivered from the optimization routine for calculation of frequency scatter shown in Fig. 6. Thus, the effect of the geometry to the frequency lift can also be investigated using the results of a maximum/minimum frequency optimization.

The main driver for this investigation is the question how standstill frequency scatter of actual geometries is transformed to rated speed operation. In particular, this knowledge is useful for definition of standstill allowable ranges. Following the procedure

1. Search for geometries providing a standstill band
2. Search for geometries providing a rated speed band
3. Feed the geometries of 1. to the rated speed SEQ
4. Feed the geometries of 2. back to the standstill SEQ

a cross comparison of the frequency lift for the identified geometries can be conducted

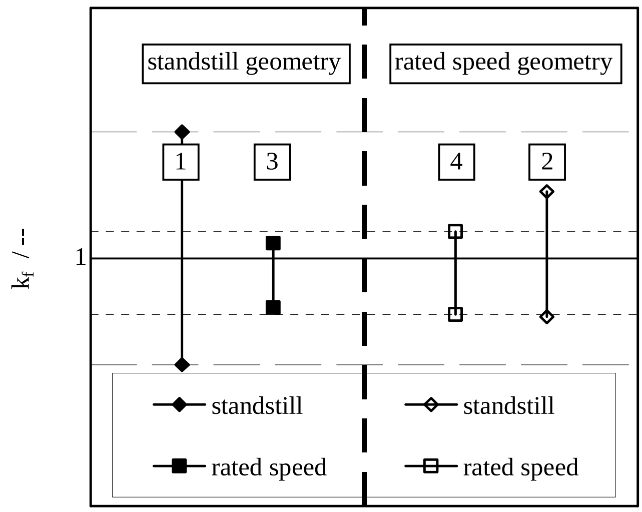

FIGURE 15 CROSS-GEOMETRY EVALUATION FOR ONE MODE

Figure 15 shows the result of this procedure for one real airfoil geometry. On the left side of the diagram the scatter bands of geometries identified to lead to a maximum standstill deviation are shown at standstill and rated speed condition.

Meanwhile, the right side shows the bands for the maximum band rated-speed-geometries at the different rotor speeds. The comparison should be done on the pairs 1 / 2 and 3 / 4. It can be seen that the frequency width of the band for the actual optimized rotor speed includes the frequency band of the re-fed geometry (i.e. 1 includes 2 and 4 includes 3). This has to be expected, as the identified geometry leads to a maximum frequency deviation at the optimization operating condition and the design space for the optimization routine is the same for both runs.

The shown behavior leads to interesting conclusions

- A blade which shows a high frequency profile in standstill must not necessarily be the blade with highest frequencies of the whole ring at nominal conditions.
- The frequency scatter width of a population tightens during speed up from standstill to rated speed.
- The frequency difference of standstill frequencies of two blades is probably not the same at rated speed.

Comparison of Blade Designs

Finally, the predicted frequency bands for two different blade design types are discussed. One of the designs is shown in Fig. 1. The other one is of similar size and shape.

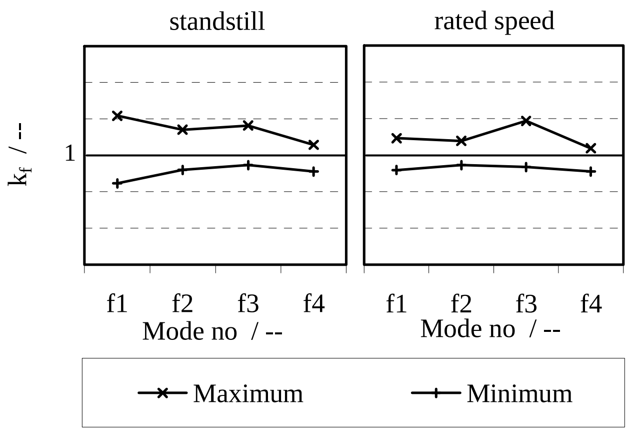

FIGURE 16 FREQUENCY BANDS IN STANDSTILL AND RATED SPEED FOR BLADE DESIGN A

Figure 16 shows the calculated relative frequency bands for the first four natural frequencies of blade design A. The normalized frequency deviation factor was calculated using Eq. (14). According to this, the nominal geometry is assigned to a value of “1” by definition. The scaling of both abscissas in Fig. 16 and Fig. 17 is kept constant for direct comparisons. At standstill, design A tends to higher frequencies than the nominal design, leading to an asymmetrically distributed scatter range. This asymmetry is increased under rated speed conditions. Furthermore, it can be seen that the overall width for all frequencies is significantly reduced at rated speed. The same data for design B is shown in Fig. 17. At a first glance both designs behave similar. In contrast to type A the second design reveals a reduced overall frequency spread. Especially at standstill conditions, but also at rated speed.

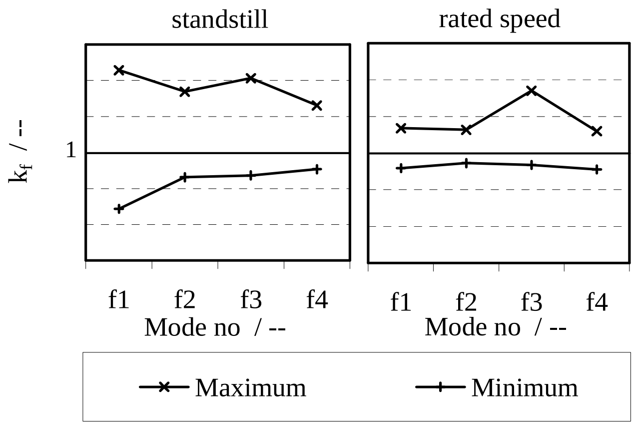

FIGURE 17 FREQUENCY BANDS IN STANDSTILL AND RATED SPEED FOR BLADE DESIGN B

CONCLUSIONS

This work describes a procedure for prediction of frequency scatter ranges for realistic geometries of freestanding last stage steam turbine blades. All required input data is a FE model of the nominal geometry and geometric tolerance data. As this information is available during the development process of a new blade design, this procedure can be used for predicting expected frequency bands at this time.

The underlying simplified model is based on a deterministic matrix equation. The chosen mathematical description provides benefits for the subsequent application of the equations in optimization algorithms.

It is shown by comparing FE calculated and predicted frequency deviations that the formulation of the simplified equation is a reasonable and accurate model for the prediction of frequency scatter and tolerance definition.

The combination of the simplified equation with a constraint minimization algorithm can be used for identification of potential frequency scatter ranges. All required constraints can be derived from physical entities.

The procedure is expanded by wrapping the inner routine with another minimization algorithm, which allows the identification of a geometric tolerance satisfying predefined frequency limits under standstill or rated speed operation. The allowable frequency deviation can be defined by the tuning of the nominal geometry and safety margins against the rotor harmonics.

In a next step, the implemented algorithms are used for analyzing the frequency lift behavior of one blade design. It is shown that the small geometric deviations influence natural frequencies at standstill and at rated speed conditions as well as the frequency lift behavior.

Finally, the potential of the described method is shown by comparing two different blade designs. As a result, it can be stated that the potential frequency scatter ranges represent a unique footprint for a specific blade design.

Permission for Use:

REFERENCES

[1] Stüer, H., Hermeler, J.,Richter,,C., Bettentrup, J., Deckers,M. 2006, “Entwicklung von neuen Beschaufelungen zur Wirkungsgradsteigerung von Niederdruck-Dampfturbinen“, Conf. Proc. Kraftwerks-technisches Kolloquium Dresden, 2006

[2] Gloger, M., Neumann, K., Termuehlen, H., 1986, “Design Criteria for Reliable Low-Pressure Blading”, ASME 86-JPGC-Pwr-42 , pp. 1-9

[3] Martel, C., Corral. R., Llorens, J., 2006, “Stability Increase of Aerodynamically Unstable Rotors Using Intentional Mistuning.” ASME Paper GT2006-90407, ASME Conf. Proc.2006

[4] Stueer, H., Siewert, C., 2010, “Forced Response Analysis of Mistuned Turbine Bladings”, ASME Paper GT2010-23782, ASME Conf. Proc.2010

[5] Moeckel, C., Darmofal, D., Kingston, T., Norton, R, 2007, “Toleranced Designs of Cooled Turbine Blades Through Probabilistic Thermal Analysis of Manufacturing Variability”, ASME Paper GT2007-28009, ASME Conf. Proc. 2007

[6] Wei Duan, Zhang-Qi Wang, 2007, “Probabilistic Analysis of Static Frequency and Dynamic Frequency of Steam Turbine Blade Based on RBF Neural Network and Monte Carlo Simulation”, Int. Conf. on Machine Learning and Cybernetics 2007 , Vol. 6, pp. 3512-3517, IEEE 2007 ISBN 978-1-4244-0973-0

[7] Nelles O., 2001, ”*Nonlinear System Identification*“, Springer, Berlin, ISBN 3-540-67369-5

